Bone 47 (2010) 117–126

Contents lists available at ScienceDirect

Bone

journal homepage: www.elsevier.com/locate/bone

The association of human mesenchymal stem cells with BMP-7 improves bone regeneration of critical-size segmental bone defects in athymic rats

Giorgio Burastero [a,1], Sonia Scarfì [b,c,*,1], Chiara Ferraris [b], Chiara Fresia [c], Nadia Sessarego [d], Floriana Fruscione [b], Francesco Monetti [e], Francesca Scarfò [e], Peter Schupbach [f], Marina Podestà [d], Guido Grappiolo [a], Elena Zocchi [b,c]

[a] Hip Surgery Unit and "Livio Sciutto" Foundation, S. Corona Hospital, Pietra Ligure, Italy
[b] Advanced Biotechnology Center, Genova, Italy
[c] Department of Experimental Medicine, Section of Biochemistry, and Center of Excellence for Biomedical Research, University of Genova, Italy
[d] Stem Cell Center, S. Martino Hospital, Genova, Italy
[e] Department of Diagnostic Imaging, National Institute for Cancer Research, Genova, Italy
[f] Research Laboratory for Implants and Biomaterials, Horgen, Switzerland

ARTICLE INFO

Article history:
Received 2 December 2009
Revised 25 March 2010
Accepted 25 March 2010
Available online 1 April 2010

Edited by: Thomas Einhorn

Keywords:
Human MSC
BMP-7
Osteogenic differentiation
Rat model
Orthoss

ABSTRACT

Critical size segmental bone defects are still a major challenge in reconstructive orthopedic surgery. Transplantation of human mesenchymal stem cells (hMSC) has been proposed as an alternative to autogenous bone graft, as MSC can be expanded *in vitro* and induced to differentiate into bone-regenerating osteoblats by several bone morphogenetic proteins (BMP).

The aim of this study was to investigate whether the association of hMSC and BMP-7, with providing the necessary scaffold to fill the bone loss, improved bone regeneration in a rat model of critical size segmental bone defect, compared to treatment with either hMSC or BMP-7 and the matrix. In addition, we tested whether pre-treatment of hMSC with cyclic ADP-ribose (cADPR), an intracellular Ca^{2+} mobilizer previously shown to accelerate the *in vitro* expansion of hMSC (Scarfì S et al, Stem Cells, 2008), affected the osteoinductive capacity of the cells *in vivo*.

X-ray analysis, performed 2, 10 and 16 weeks after transplantation, revealed a significantly higher score in the rats treated with hMSC and BMP-7 compared to controls, receiving either hMSC or BMP-7. Microtomography and histological analysis, performed 16 weeks after transplantation, confirmed the improved bone regeneration in the animals treated with the association of hMSC and BMP-7 compared to controls. Pre-treatment with cADPR to stimulate hMSC proliferation *in vitro* did not affect the bone regenerating capacity of the cells *in vivo*.

These results indicate that the association of *in vitro* expanded hMSC with BMP-7 provide a better osteoinductive graft compared to either hMSC or BMP-7 alone. Moreover, cADPR may be used to stimulate hMSC proliferation *in vitro* in order to reduce the time required to obtain a transplantable number of cells, with no adverse effect on the bone regenerating capacity of hMSC.

Introduction

Large bone defects can be caused by trauma, disease or developmental defects and the surgical treatment of critical size bone loss is a major challenge to the reconstructive surgeon. Autogenous bone grafts require harvest of bone from an intact site and are burdened by complications at both the harvest and graft sites [1]. An alternative, emerging strategy to bone transplantation for the treatment of large bone defects is tissue engineering, through the use of bone-regenerating stem cells embedded in a bio-compatible matrix [2]. Mesenchymal stem cells (MSC) are a rare population of non-hematopoietic cells present in the bone marrow (BM) that can be expanded *in vitro* and induced to differentiate into several mesodermal cell types, including osteoblasts and chondrocytes [3]. BM-derived MSC seeded onto hydroxyapatite and implanted into non-obese diabetic/severe combined immunodeficiency (NOD/SCID) mice have been shown to induce new bone formation [4]. Subsequent studies have demonstrated the bone-regenerating capacity of *in vitro* expanded and *in situ* implanted MSC in several animal models of critical segmental bone defects [5–7]. These results have led to the approval of clinical trials for the implantation of human MSC (hMSC)-matrix composites for the treatment of large bone defects in humans [8]. A major hurdle to the use of autologous or allogeneic hMSC for

* Corresponding author. Department of Experimental Medicine, Section of Biochemistry, University of Genova, Viale Benedetto XV, no 1, 16132, Italy. Fax: +39 010354415.
E-mail address: soniascarfi@unige.it (S. Scarfì).
[1] These Authors contributed equally to the work.

8756-3282/$ – see front matter © 2010 Elsevier Inc. All rights reserved.
doi:10.1016/j.bone.2010.03.023

stem cell-based bone repair is the need for large cell numbers: the low frequency ($1/10^5$) of hMSC in the BM-derived cell suspensions used as a source of stem cells and the long time required for their *in vitro* expansion (several weeks) under stringent culture conditions [9] lead to high production costs.

The matrix to be used in association with the *in vitro* expanded hMSC in the bone graft should, (i) provide initial physical support for the transplanted cells inside the bone defect, and, (ii) release chemical signals stimulating osteoblast differentiation [10]. Regarding physical support, among the wide range of organic and inorganic osteoinductive matrices tested *in vitro* and *in vivo*, particles of natural bone mineral (Orthoss®) have been shown to provide an excellent, biocompatible substrate, also amenable to remodelling during the bone regeneration process [11–13]. Osteoblast differentiation is known to be regulated by bone morphogenetic proteins (BMPs), which are members of the Transforming Growth Factor (TGF) superfamily, and BMP-2 and BMP-7 (also known as osteogenic protein-1) are currently used clinically to stimulate new bone formation [14]. Most recently, BMP-7 has been shown to be primarily responsible for the *in vitro* osteoblastic differentiation of primary hMSC, by inducing the expression of osteoblast-associated genes and matrix mineralization independently of BMP-2 expression [15].

The scope of this research was to assess the osteoinductive capacity of the association of *in vitro* expanded hMSC and BMP-7 using as the matrix support in an athymic rat model of critical size segmental bone defect. In addition, as it has been recently demonstrated that cyclic ADP-ribose (cADPR), a universal intracellular calcium mobilizer, stimulates the *in vitro* expansion of human MSC [16], we investigated whether pre-treatment with cADPR affected the *in vitro* differentiating ability and/or the *in vivo* osteoinductive capacity of expanded hMSC.

Materials and methods

Materials

Orthoss®, natural bone mineral spongiosa granules of 0.25–1 mm particle size, was purchased from Geistlich Biomaterials, Wolhusen, Switzerland. Human recombinant BMP-7 (hrBMP-7) (OP-1 implant, insoluble) was purchased from Stryker Biotech, Rome, Italy: each vial contains a combination of 3.3 mg hrBMP-7 and 1 g of purified Type I bovine collagen.

Animals

Male athymic rats (Harlan HSD: Rh-rnu, median weight, 379 g) were purchased from Harlan Italy (S. Pietro al Natisone, Udine, Italy). In skeletally mature animals (2 months old), a critical size segmental bone defect (CSSBD) was produced. The *in vivo* experimental protocol was approved by the Italian Ministry of Health and by the Animal Care and Use Committee of the Advanced Biotechnology Center, Genova, Italy, where the experimentation was performed. All experiments were conducted in accordance with international standards on animal welfare and adequate measures were taken to minimise pain or discomfort.

Isolation and culture of human mesenchymal stem cells

Human MSC (hMSC) were purified from samples of bone marrow and bone fragments obtained from the acetabulus of patients undergoing hip arthroplasty, after written consent and under the approval of the S. Corona Hospital ethics committee. At least 50 ml per sample were collected from 6 patients, age 59 to 73 (2 males, 4 females). Mononuclear cells (MNC) were isolated by centrifugation on Ficoll Paque Plus (Amersham Bioscience, Milan, Italy) and then plated on 175 cm^2 flasks, at 2×10^5 cells/cm^2 in McCoy Medium (Lonza, Milan, Italy) supplemented with 10% of FBS (from selected lots, Invitrogen, Milan, Italy) and with 100 U/ml penicillin plus 100 µg/ml streptomycin. After 48 h culture, the medium was removed and fresh medium was added to each flask. Cells were maintained at 37 °C in a humidified atmosphere with 5% CO_2 and half of the medium was changed every 3 days. Cell confluence usually was reached in two weeks, this being considered passage #0: cells were then expanded (1:4) and cultured as described. At passage #2 cells were deep frozen until use for implantation.

Cell proliferation assay

For the proliferation assay, hMSC were plated at a density of 5×10^3 cells/well in 96-well plates and allowed to adhere overnight. The day after, 0.2 or 1 µg/ml hrBMP-7, 2 or 10 µM cADPR, or 1 µg/ml hrBMP-7 and 10 µM cADPR in combination were added to the cells, in quadruplicate. After 24 or 48 h culture, the MTT test was performed to evaluate the extent of cell proliferation [17].

Differentiation and gene expression analysis

Cells were plated at a density of 3×10^5 cells in 35 mm-culture dishes and incubated in complete medium in the presence or absence of 1 µg/ml BMP-7 or of 1 µg/ml BMP-7 and 30 µM cADPR for 48 h. Following this treatment cells were induced to differentiate in the presence of 10 mM 2-glicerol phosphate, 10 µM dexamethasone and 50 µM ascorbic acid in DMEM-F12 medium supplemented with 10% FCS and penicillin plus streptomycin (osteocyte differentiation medium, ODM). Fresh medium and osteogenic factors were replaced every 3 days. After 1 week, total RNA was extracted using a RNeasy Micro Kit (Qiagen, Milan, Italy) according to the manufacturer's protocol including DNase treatment. Quality and quantity of RNA were analyzed using a NanoDrop spectrophotometer (Nanodrop Technologies, Wilmington, DE, USA). The cDNA was synthesized from 200 ng of total RNA with the iScript cDNA Synthesis Kit (Bio-Rad Laboratories, Milan, Italy). Each RNA sample was controlled for genomic DNA contamination without reverse transcriptase addition into cDNA synthesis mixture. Quantitative real-time PCR amplification was performed in triplicate using the Bio-Rad IQ5 instrument (Bio-Rad) and the 2×iQ Custom Sybr Green Supermix (Bio-Rad). The 20 µl PCR mixture contained 2 µl of diluted cDNA and 0.2 µM of each primers. All samples were amplified in triplicate and the mean was used for RT-qPCR analysis. Statistical analyses of the qPCR were obtained using the iQ5 Optical System Software version 1.0 (Bio-Rad) based on the ΔΔCt method [18,19]; relative expression levels were normalized on GAPDH (reference gene). For each specific primers set the efficiency was >95% and a single product was seen on the melting curve analysis. Specific primers for Alkaline phosphatase (ALP, NM_000478), osteopontin (OPN, NM_000582) and Runt-related transcriptional factor 2 (Runx2, NM_004348) were designed through Beacon Designer 2.0 Software (Bio-Rad) and are listed in Table 1.

Table 1
Primers used for real-time PCR.

Target gene	Accession number	Sequence	Product (bp)
ALP	NM_000478	5′-ATGAGGCGGTGGAGATGG-3′ 5′-ATACAGGATGGCAGTGAAGG-3′	196
RUNX 2	NM_0004348	5′-CCAGCAGCACTCCATATCTCTAC-3′ 5′-CATCAGCGTCAACACCATCATTC-3′	176
OPN	NM_000582	5′-CTGATGAATCTGATGAACTGGTC-3′ 5′-GTGATGTCCTCGTCTGTAGC-3′	192
GADPH	NM_002046	5′-CCTGTTCGACAGTCAGCCG-3′ 5′-CGACCAAATCCGTTGACTCC-3′	101

Preparation of the graft

For the preparation of graft implants 2×10^6 frozen hMSC at passage #2, were rapidly thawed in a water bath at 37 °C and then immediately plated in a 175 cm^2 flask and incubated for 48 h at 37 °C in a humidified atmosphere with 5% CO_2 in the presence or absence of 30 μM cADPR. After 48 h cells were detached from the flasks, counted and then 2×10^6 of untreated or cADPR-treated hMSC were centrifuged at 400*g* for 5 min. Cells were then resuspended in 100 μl of PBS containing 10 mM glucose (PBS-glucose) and immediately used to prepare the implants. 100 μl of PBS-glucose, with or without hMSC, was mixed with Orthoss®, with hrBMP-7 (when present) and with approximately 200 μl of 2% carboxymethyl cellulose-based hydrogel (Sigma). For hMSC dose finding experiments, 0.5, 1, 2, 3 or 6×10^6 cells were transplanted in the presence of 120 mg Orthoss® and 80 μg hrBMP-7. 2×10^6 hMSC were used in all subsequent experiments, and the following graft composition was utilized in the five animal groups studied: group #1, 120 mg Orthoss®; group #2, Orthoss® and 80 μg hrBMP-7; group #3, Orthoss® and hMSC; group #4, Orthoss®, hMSC and hrBMP-7; group #5, Orthoss®, cADPR-pre-treated hMSC and hrBMP-7.

hMSC migration from the graft in vitro

To evaluate the ability of hMSC to migrate out of the graft, the same implant employed for experimental group #4 (see "preparation of the graft") was cultured on 35×10 mm dishes in 1 ml complete medium and incubated in a humidified atmosphere at 37 °C. At various times, the medium was removed and live cells were stained with 2.5 μM calcein green (Molecular Probes, Invitrogen, Milan, Italy) in 1 ml of Hank's balanced salt solution (HBSS, Sigma) for 30 min at 37 °C. The dishes were then washed twice with HBSS and immediately analysed under a confocal microscope (Leica TCS SL) equipped with argon/He–Ne laser sources and a HC PL FLUOTAR 20.0×0.5 air objective. Laser energy of the 488 nm line was set at 20%. Data were acquired in an emission range of 500–580 nm, while the photo-multiplier voltage gain was set to eliminate autofluorescence of cells in the same interval of acquisition. Z-stacks of 220 sections with a Z-step of 820 nm for a total thickness of 180 μm were acquired, starting from the plastic surface of the dish. 3-D projections of the micrographs were obtained using the Leica LCS software and a color-code was applied to show the thickness of the samples.

Rat model of critical size segmental bone defect

In this study, CSSBD were surgically created in the right hind limb of male athymic rats. For hMSC dose finding experiments four rats per experimental group were used for a total of six groups differing for the number of hMSC employed, while in the following experiments six animals per group were used (the above mentioned groups #1–5). Rats were operated under general anaesthesia, achieved with the intraperitoneal injection of diazepam (1 mg per 100 g of body weight) and the intramuscle administration of Xilazine (0.5 mg per 100 g of body weight) and Ketamine (4 mg per 100 g of body weight).

The right limb was shaved and prepared. The anterior surface of the right femur was exposed from the antero-lateral side, saving muscles and tendons. Before femoral osteotomy, a 3-mm thick and 25-mm long polymethyl-methacrylate plate was fixed with four stainless steel cerclage wires. Then, a femoral gap of 6 mm was cut in the central diaphysis and filled with the graft, prepared as described above. Unprotected weight bearing was allowed immediately after the operation.

Evaluation of bone regeneration

Bone regeneration was evaluated by X-ray with a direct digital mammography equipment, (Giotto Image-MD by IMS, Bologna, Italy) on animals under general anaesthesia 2, 10 and 16 weeks after transplant. Radiographs were scored by two independent observers according to a modified Cook classification [20], the modification consisting in the addition of score #6, indicating overgrowth ossification. At 16 weeks from the transplant, animals were sacrificed and the operated femurs were harvested, dissected free of the surrounding muscle tissue and fixed in 10% formaldehyde in PBS. The specimens were scanned using a high resolution micro-CT system (μCT 40, Scanco Medical, Bassersdorf, Switzerland) in multislice mode. Each image data set consisted of approximately 600 micro-CT slice images. Data were acquired in high-resolution mode with an x-, y-, z-resolution of 16 μm. The image data sets were used, (i) to produce 3-D views of the specimens, using a dedicated software (Scanco Medical, Switzerland), and (ii) to quantify the percentage of new bone and of Orthoss®. Since bone has a lower degree of mineralization than Orthoss®, the two materials can be distinguished by their grey levels in Micro-CT scans. The threshold was set at 200 for bone and 340 for Orthoss®. Finally, fixed samples were processed for the preparation of non-demineralized ground sections according to the technique of Donath and Breuner [21]. Briefly, specimens were dehydrated and the blocks were infiltrated with Technovit 7200 VLC-resin (Haereus Kulzer Gmbh, Wehrheim, Germany). Infiltrated specimens were then placed into embedding molds, and polymerization was performed under UV-light. Polymerized blocks were sliced longitudinally on an Exakt cutting unit (Exakt, Norderstedt, Germany). The slices were reduced by microgrinding and polishing using an Exakt grinding unit to an even thickness of 30–40 μm. Sections were stained with toluidine blue/pyronine G and examined using both a Leica MZ16 stereomicroscope (Leica Microsystems srl, Milan, Italy) and a Leica 6000DRB light microscope.

In order to quantify the connective and hemopoietic tissues, Orthoss® and new bone, in each histological section (2 sections per animal, 6 animals per experimental group) the area corresponding to each tissue type in the femoral gap was measured with the Adobe Photoshop 7.0 Professional software.

Statistical analysis

Data are presented as mean ± standard deviation (SD) of mean. Student's *t*-test was used to analyse the difference between two groups. Analysis of variance (ANOVA) and multi-comparison analysis using Tukey's test were performed on the data in Figs. 4B and 5B. $p<0.05$ was considered statistically significant.

Results

Effect of BMP-7 and cADPR on the in vitro proliferation of hMSC

Prior to starting the *in vivo* experimentation, we preliminarily tested the effect of human recombinant BMP-7 (hrBMP-7) and of cADPR on the proliferation of hMSC *in vitro*. hrBMP-7 and cADPR were added to cultured hMSC at concentrations known from the literature to exert stimulatory effects on cell differentiation [15] and proliferation [16], respectively. At 0.2 and 1.0 μg/ml, hrBMP-7 slightly reduced the cell number after 24 and 48 h culture compared to untreated controls (Fig. 1), in line with the reported transient attenuation of the cell cycle induced by the differentiating factor [15]. Conversely, cADPR (2 and 10 μM) slightly stimulated cell proliferation in a concentration-dependent manner, the highest concentration inducing a 40% increase of the cell number after 48 h culture (Fig. 1), similarly to what already reported [16]. The effect of hrBMP-7 on hMSC previously expanded for 48 h in the presence of cADPR was also explored, as this schedule of cell treatment was to be subsequently employed for the *in vivo* experimentation in one of the rat groups. The reduction of the cell number induced by 1 μg/ml hrBMP-7 after 24 and 48 h compared to controls, pre-treated for 48 h

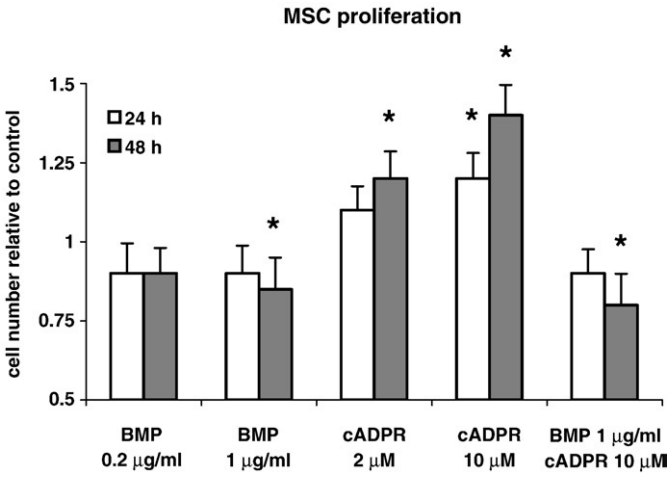

Fig. 1. Effect of hrBMP-7 and cADPR on hMSC proliferation *in vitro*. hMSC proliferation was evaluated by MTT assay in cells treated with hrBMP-7 and/or cADPR at the indicated concentrations for 24 h (white bars) or 48 h (grey bars). Histograms represent the mean ± SD from three independent experiments, performed in quadruplicate. $^{*}p<0.05$ compared to control, untreated cells.

with cADPR and then cultured without addition of hrBMP-7, was similar to that observed when hrBMP-7 was added to cADPR-untreated cells (Fig. 1), indicating that hMSC expanded in the presence of cADPR were also subject to the cell cycle attenuating effect of BMP-7.

Effect of BMP-7 and cADPR on transcription of osteogenic differentiation marker genes

We also tested the effect of hrBMP-7 and of cADPR on the osteogenic differentiation capacity of hMSC *in vitro*. hMSC were cultured in complete medium for 48 h in the presence or absence of BMP-7, alone or together with cADPR. Cells were then induced to differentiate for 1 week in ODM and total mRNA was extracted and qPCRs were performed to quantify expression of the following osteogenic differentiation marker genes: Runt-related transcriptional factor 2 (Runx2), alkaline phosphatase (ALP) and osteopontin (OPN). Results are summarized in Fig. 2; an increased transcription of all marker genes was indeed observed in ODM-treated cells (C, white bars) compared to controls, maintained in medium without differentiating factors (C, grey bars). Expression of Runx2 in hMSC pre-treated with hrBMP-7, with or without cADPR, was similar to that observed in the differentiated control (Fig. 2A, white bars). Conversely, expression of both ALP and OPN significantly increased in cells pre-treated with hrBMP-7, without or with cADPR, compared to the respective differentiated controls (Fig. 2B–C, white bars). In cells allowed to differentiate for 2 weeks, however, expression of OPN in the differentiated control increased to levels similar to those observed in the presence of hrBMP-7, suggesting that the growth factor accelerated OPN gene induction by the differentiating medium (not shown). Surprisingly, upregulation of Runx2 (3.1 folds) and OPN (2.7 folds) was also observed in the absence of ODM, in cells pre-treated with hrBMP-7 and cADPR compared to untreated controls and to cells incubated with hrBMP-7 alone (Fig. 2A–C, grey bars), suggesting that the combination of cADPR and the bone morphogenetic protein could induce the expression of osteogenic markers in the absence of differentiating factors.

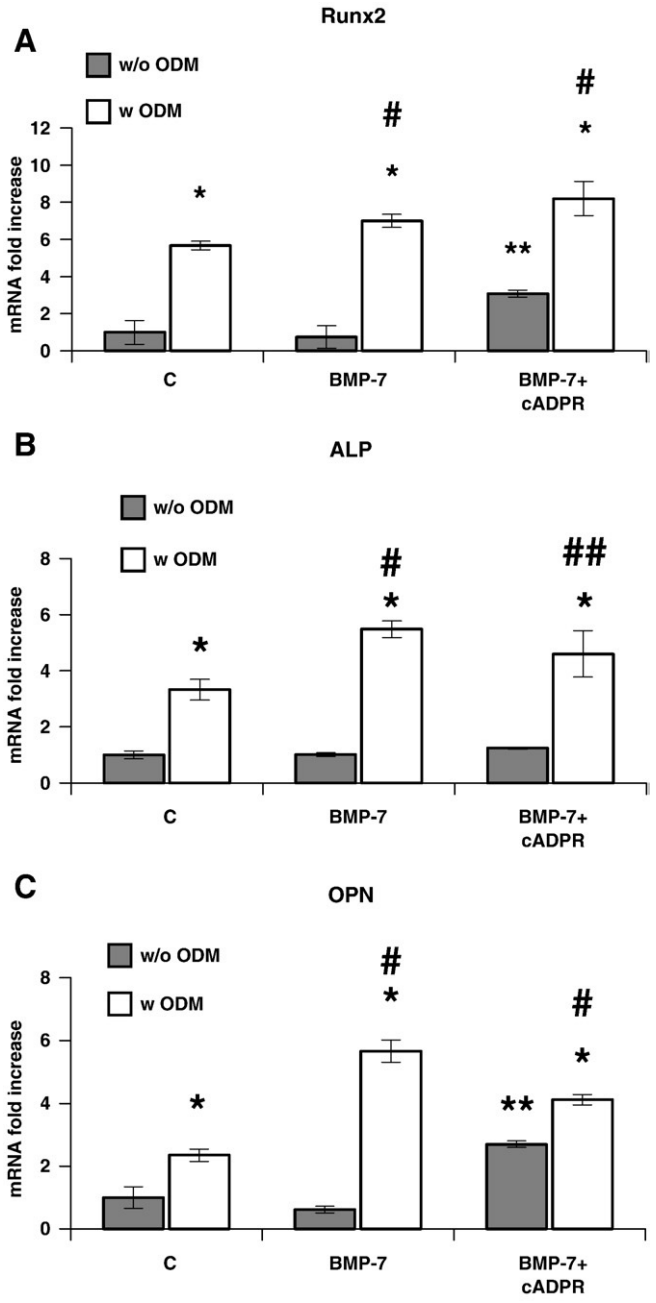

Fig. 2. Expression of Runx2, ALP and OPN in differentiated and undifferentiated hMSC. RT-qPCR of Runx2 (panel A), ALP (panel B) and OPN (panel C) genes expressed in hMSC pre-treated or not with hrBMP-7 alone or in combination with cADPR (hrBMP-7+ cADPR) and cultured in the presence (white bars) or absence (grey bars) of osteocyte differentiating medium (ODM) for 1 week. Results are expressed as mRNA fold increase, normalized on the reference gene (GAPDH) and compared to control, undifferentiated cells. Histograms represent the mean ± SD of three independent experiments, performed in triplicate. Panel A: $^{*}p<0.0005$ compared to the same sample w/o ODM (grey bar); $\#p<0.0005$ compared to control with ODM (C, white bar); $^{**}p<0.0025$ compared to control w/o ODM (C, grey bar). Panel B: $^{*}p<0.0005$ compared to the same sample w/o ODM (grey bar); $\#p<0.0005$ compared to control with ODM (C, white bar); $\#\#p<0.05$ compared to control with ODM (C, white bar). Panel C: $^{*}p<0.0005$ compared to the same sample w/o ODM (grey bar); $\#p<0.0005$ compared to control with ODM (C, white bar); $^{**}p<0.0005$ compared to control w/o ODM (C, grey bar).

hMSC migration out of the graft in vitro

The same type of implant employed for experimental group #4 (hMSC, Orthoss® and rhBMP-7) was incubated at 37 °C on Petri dishes and, at various times, live cells were stained with the cytoplasmatic marker calcein green and examined by confocal microscopy to visualize cells migrated from the implant and attached to the plastic surface and cells still inside the Orthoss® particles. Artificially coloured 3-D projections were obtained with the Leica software. Indeed, hMSC were able to migrate out of the graft as early as 4 h after the onset of culture (not shown). After 24 h incubation of the implant,

hMSC were found both out of the implant, attached to the plastic surface underneath the Orthoss® particles (purple cells), and inside the implant, at various heights, as documented by the green-yellow-red colour attributed by the software to cells present at increasing distances from the plastic surface (Fig. 3A).

To determine if leakage of BMP-7 occurred from the graft, the same type of implant employed for experimental group #3 (Orthoss® and rhBMP-7) was incubated in 1 ml HBSS at 37 °C for up to 24 h. Release of BMP-7 into the medium could not be detected by dot-blot analysis, using a specific anti-human BMP-7 goat polyclonal antibody. These results are in agreement with *in vivo* studies with radiolabeled OP-1, demonstrating very limited systemic release of the protein (European Public Assessment Report, Product Information Osigraft-H-C-293-II-38, April 2, 2008).

Dose-finding of hMSC for bone repair in the rat model

In order to determine the minimum number of hMSC capable of producing a radiographically appreciable bone regeneration at the site of the bone defect, different numbers of hMSC were transplanted with 80 µg of hrBMP-7 in a matrix of Orthoss® (120 mg). Radiographs taken 12 weeks after transplantation and scored according to Cook showed a dose-dependent increase of the score up to 2×10^6 cells, while grafting of higher hMSC numbers (up to 6×10^6 cells) did not result in a further increase of the radiographic score (Fig. 3). Thus, the minimum cell number producing the highest radiographic score of bone regeneration (2×10^6 cells) was subsequently employed in the animal experimentation. In another set of experiments, increasing amounts of hrBMP-7 were tested for their efficacy in combination with a fixed number (2×10^6) of hMSC. No significant radiological differences were observed 12 weeks post-operatively between animals (4 per group) treated with 80 or 160 µg of rhBMP-7 (not shown). Thus, 80 µg of hrBMP-7 were used in the subsequent animal experimentation.

Radiographic evaluation of bone repair in the rat model

At 2 weeks postoperatively, no significant radiographic evidence of bone repair was observed in any one of the experimental groups (Fig. 4A, panel a shows a representative image). After 16 weeks, still no or minimal radiographic evidence of bone repair was observed in group #1 (Orthoss® only, Fig. 4A, panel b) and #2 (Orthoss® with hMSC, Fig. 4A, panel c), while all other groups showed evidence of new bone formation, with a score increasing from group #3 (Orthoss® and hrBMP-7, Fig. 4A, panel d), to groups #4 (Orthoss®, hMSC and hrBMP-7, Fig. 4A, panel e) and #5 (Orthoss®, cADPR-treated hMSC and hrBMP-7, Fig. 4A, panel f). In particular, all of the animals in groups #4 and #5 had a Cook score ≥3 (presence of new bone of cortical density at both ends of the bone defect) and 2 out of 6 animals had a score of 5 (loss of graft-host distinction with significant new bone remodelling). Group #3 (Orthoss® and hrBMP-7) scored significantly lower than groups #4 and #5, yet better than groups #1 and 2, with 5 out of 6 animals showing new, albeit disorganized, bone bridging the graft to both ends of the bone defect (evaluation score 2). Fig. 4B summarizes the evaluation scores of the five experimental groups.

To gain more information regarding the structure of the graft inside the bone defect, a µCT analysis was performed at 16 weeks postoperatively on fixed bone samples from each experimental group, enabling the identification of the new bone and of the bone substitute used as the matrix (Orthoss®). Results are shown in Fig. 5A. Large bone defects with no evidence of new bone formation were observed in the samples from group #1 (matrix only, in white, Fig. 5A panel a), in agreement with the radiographic evidence. Very little new bone formation (in red) was observed in the specimens from group #2 (hMSC, Fig. 5A panel b), where new bone accounted for 16% only of total bone. A significantly higher percentage of new bone compared to the previous groups was present in the grafts from group #3 (hrBMP-7,

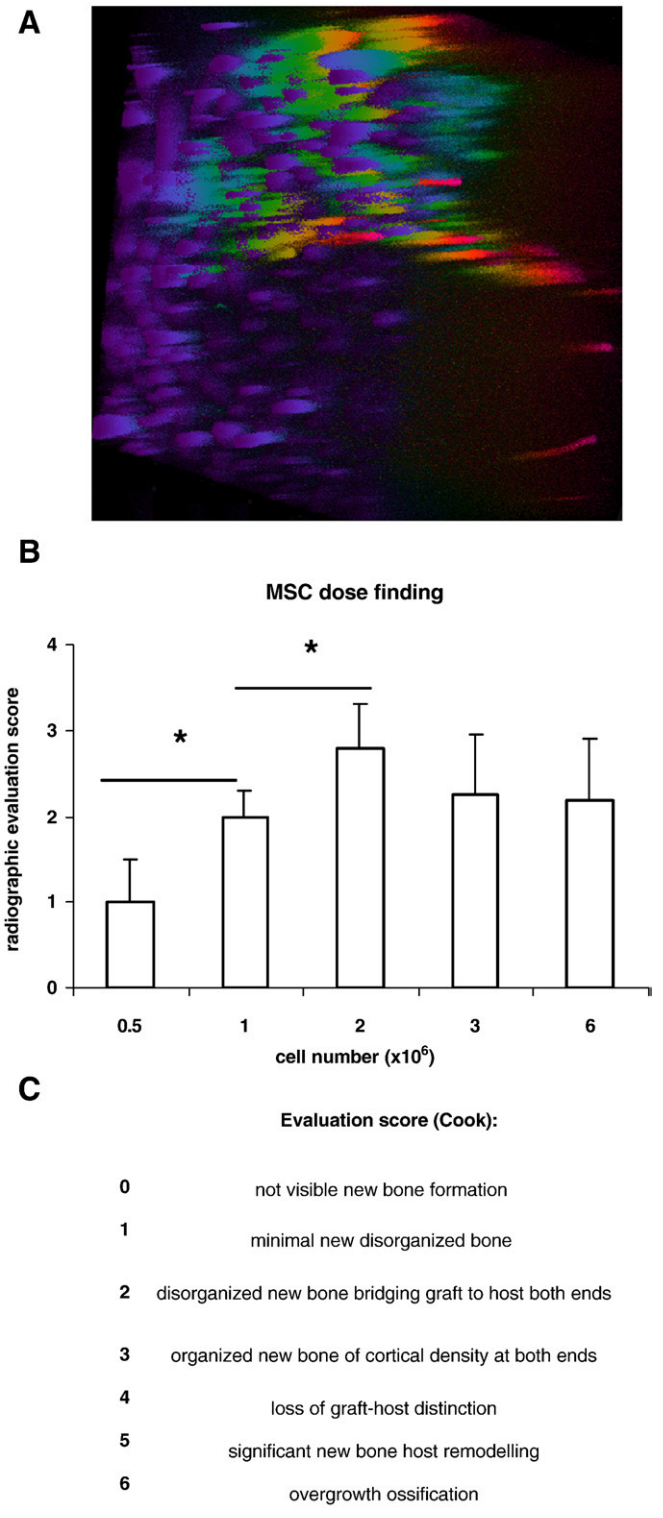

Fig. 3. Out of graft migration of hMSC in vitro and hMSC dose finding in the CSSBD rat model. hMSC migration was evaluated by confocal microcopy (panel A) after 24 h incubation of an implant containing hMSC, Orthoss® and rhBMP-7 in 1 ml complete medium on a Petri dish. After cell staining with calcein green, samples were analysed by confocal microscopy with a HC PL FLUOTAR 20.0×0.5 air objective. Z-stacks of 220 sections with a Z-step of 820 nm for a total thickness of 180 µm were taken, starting from the plastic surface. 3-D projections, artificially colored to highlight the depth of the acquisition data set, were obtained using the Leica LCS software. Cells attached to the plastic surface are purple while the blue-green-yellow-red colours indicate cells at increasing distances from the plastic surface. Radiographic evaluation scores (panel B) according to a modified Cook classification (panel C) of X-rays taken12 weeks postoperatively in athymic rats (4 animals per group), receiving the indicated numbers of hMSC, with 80 µg hrBMP-7 and 120 mg of Orthoss® matrix. Results are expressed as mean ± SD of the scores given by two independent observers. *$p<0.05$.

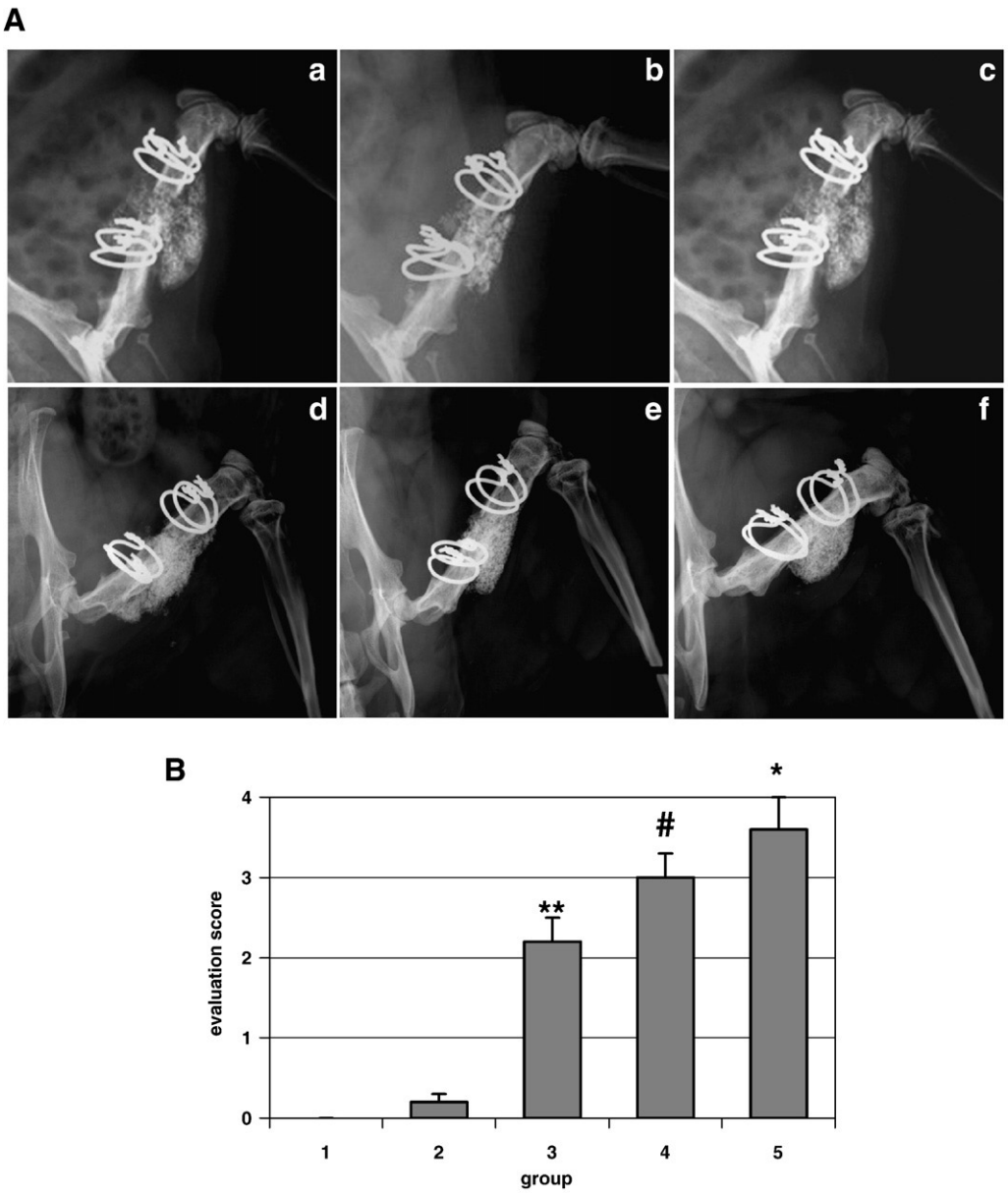

Fig. 4. Post-operative radiographic analysis of the CSSBD rat model. Panel A. X-rays were taken under general anaesthesia, with a direct digital mammography equipment (Giotto Image-MD). Representative images, taken at 2 weeks (a) or at 16 weeks (b–f) post-operatively, are shown. The following experimental groups were studied: (b) group #1 (matrix only); (c) group #2 (matrix and hMSC); d) group #3 (matrix and hrBMP-7); (e) group #4 (matrix, hMSC and hrBMP-7); (f) experimental group #5 (matrix, cADPR-pre-treated hMSC and hrBMP-7). Panel B. Radiographic evaluation scores according to a modified Cook classification (shown in Fig. 3, panel B) assigned to the X-rays taken 16 weeks postoperatively on the five experimental groups. Results are expressed as mean ± SD of the scores given to six animals per group by two independent observers. $^{**}p<0.0005$ compared to groups 1 and 2; $\#p<0.005$ and $^{*}p<0.0005$ compared to group 3, by Tukey's test.

Fig. 5A panel c), where new bone accounted for approx. 50% of total bone (Fig. 5B). The highest percentage of new bone compared to total bone (approximately 70%) was observed in the grafts from groups #4 and #5 (Fig. 5A panels d and e and B), with no significant differences between these groups. The increased bone regeneration observed in the grafts from groups #4 and #5 compared to those from group #3 is attributable to the presence of hMSC in the graft. In all cases where significant bone regeneration had occurred (groups #3, 4 and 5), a reduction of the bone matrix (Orthoss®) was also observed (Fig. 5B), indicating active Orthoss® resorption.

Histological analysis

At 16 weeks from transplant, fixed femurs from each experimental group were processed for the preparation of non-demineralized ground sections, stained with toluidine blue/pyronine G and observed through a light microscope. Images were acquired and a quantification of the areas of Orthoss®, connective tissue, new bone and bone marrow was performed. Results are summarized in Fig. 6. At 16 weeks, mainly connective tissue with very low amount of new bone was present around the Orthoss® particles filling the bone defect in animals from group #2 (hMSC), in agreement with the result of the μCT analysis (Fig. 6A, images A–B and B). Newly formed bone tissue could be detected and quantified around the matrix particles in group #3 animals (hrBMP-7), although the new bone was insufficient to fill the gap between the femoral fragments and to form a cortical callus (Fig. 6A, images C–D and B). Conversely, in the animals from groups #4 (hMSC+hrBMP-7, Fig. 6A, images E–F) and #5 (cADPR-treated hMSC+hrBMP-7, Fig. 6A, images G–H), significant amounts of new bone were observed (Fig. 6B) and were found to connect the matrix

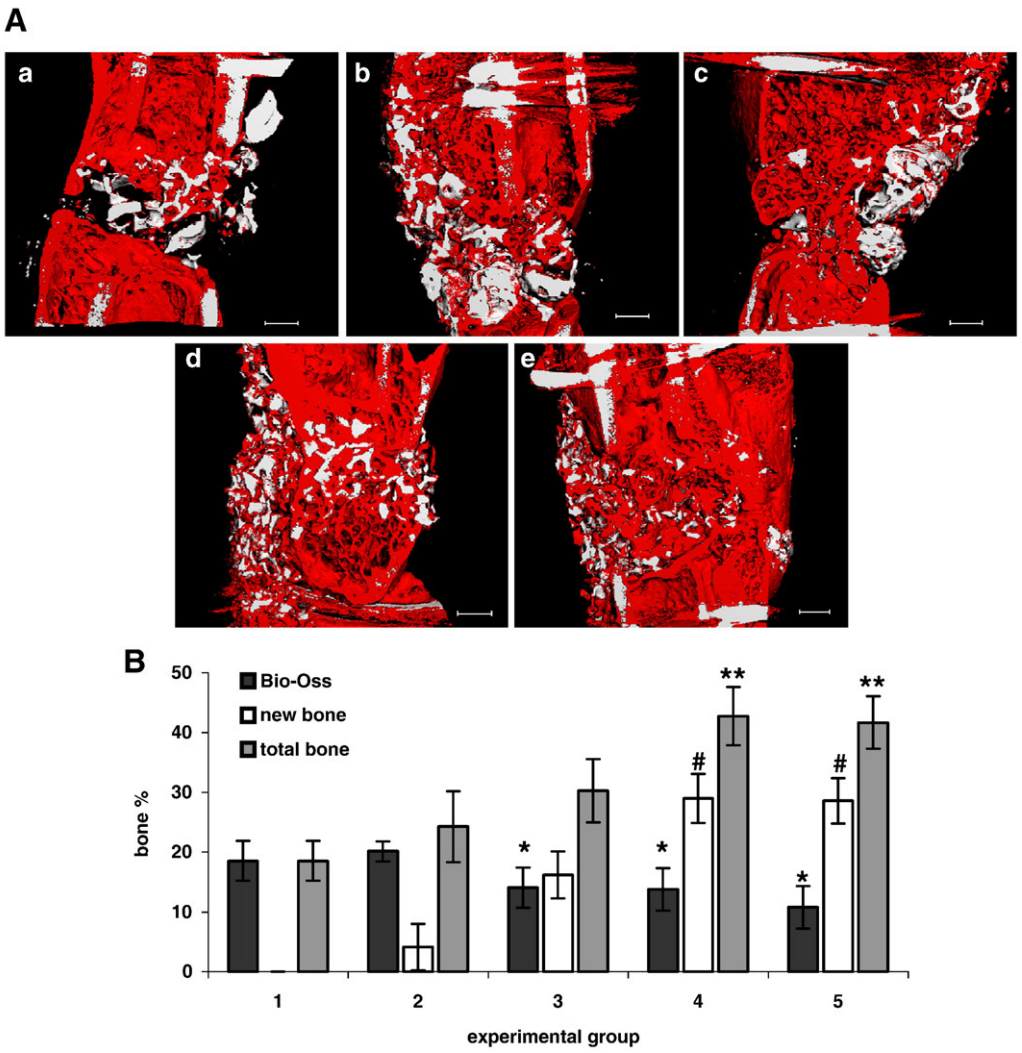

Fig. 5. µCT analysis and evaluation of new bone formation. Microtomographies were performed at 16 weeks postoperatively on the fixed femurs from each experimental group. Specimens were scanned using a high-resolution micro-CT system (µCT 40, Scanco Medical). Data were acquired in high-resolution mode and the image data sets were used to produce 3-D views of the specimens using Scanco Medical software. Panel A. A representative image for each rat experimental group is shown. Bone, including newly formed tissue, is coloured in red, while the Orthoss® matrix is colored in white. White bars span 1 mm. (a) group #1 (matrix only); (b) group #2 (matrix and hMSC); (c) group #3 (matrix and hrBMP-7); (d) group #4 (matrix, hMSC and hrBMP-7); (e) group #5 (matrix, cADPR-pre-treated hMSC and hrBMP-7). Panel B. Quantification of matrix, newly formed and total bone in the segmental bone defect area was performed on the µCT data sets from the five experimental groups, using the Scanco Medical software: black bars, matrix; white bars, new bone; grey bars, total bone. Results are the mean ± SD of 6 animals per group. $^{*}p<0.05$ compared to Orthoss® in group #1; #$p<0.025$ compared to new bone in group #3; $^{**}p<0.05$ compared to total bone in group #3, by Tukey's test.

particles inside the gap and along the cortical surface opposite to the plaque, where the matrix particles leaked from the bone defect. Furthermore, a significant bone marrow colonisation of the new bone inside the surgical gap (also quantified in Fig. 6B) was observed mainly in animals from groups #4 and #5, indicating that the regenerated bone had also regained its physiological function as hemopoietic support.

Discussion

In this study, we tested the capacity of human MSC (hMSC) together with human recombinant BMP-7 (hrBMP-7) to induce bone regeneration in an *in vivo* rat model of critical size segmental bone defect (CSSBD). The scientific literature provides extensive evidence of the osteoblastic potential of bone marrow-derived MSC from mice [22], rats [23], goats [24], pigs [25] and dogs [26], but the efficacy of hMSC in supporting bone regeneration *in vivo* is less well established. It has also been shown, both in preclinical animal studies [27] and in clinical studies [28], that hrBMP-7 has osteoinductive properties and is biologically safe [29]. Thus, *in vitro* expanded hMSC and BMP-7 have been separately used to improve bone regeneration (5–7, 27, 28): the scope of this study was to assess whether their combination further improved the healing of CSSBD. As compared to a recently published rat nonunion model, where rat MSC were cultured to form a cell sheet and then wrapped around a femur osteotomy without the need for any other support [30], in this study, the use of a biocompatible matrix was necessary to fill the large (~42 mm^3) femur gap, providing both host and donor cells with a support to grow and differentiate onto. Furthermore, Orthoss® provided a mechanically resistant support for hMSC, allowing cell adhesion without preventing cell migration (Fig. 3A), and could be partially reabsorbed under conditions of successful bone regeneration, as occurred in groups #4 and #5 (Fig. 5B), possibly allowing remodelling of the regenerated bone over time. The fact that hMSC can migrate out of the graft (Fig. 3A), while BMP-7 (OP-1 implant) is apparently retained inside the graft (see Results), confined the pro-differentiative action of BMP-7 inside the implant, while migration of transplanted hMSC apparently supported bone regeneration around the graft.

In order to test the bone regeneration capacity of hMSC in the presence of hrBMP-7, an athymic rat model was used to avoid

A

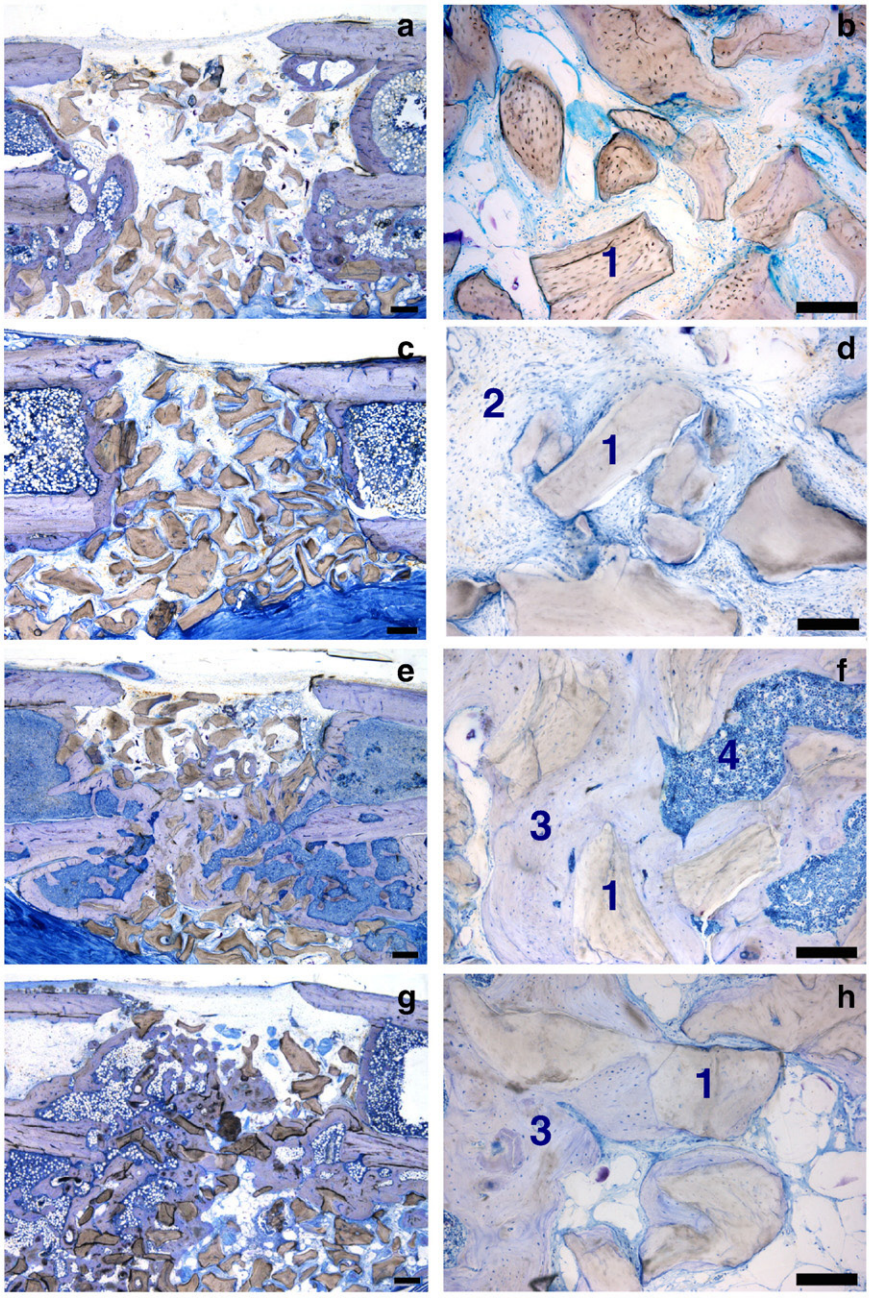

B

Experimental group	Orthoss® (1)	connective tissue (2)	new bone (3)	bone marrow (4)
#2	29±6	48±8	12±5	7±4
#3	20±5	40±9	26±7	8±5
#4	15±4	22±6	**38**±9	**21**±6
#5	16±5	17±5	**41**±8	**19**±5

Fig. 6. Histological analysis of the segmental bone defect area. Panel A: at 16 weeks postoperatively, 30 μm-thick sections of the segmental bone defect area were prepared from each specimen shown in Fig. **5**. Sections were stained with toluidine blue/pyronine G and images were taken with a Leica 6000DRB light microscope. Left column images were taken at low magnification (black bars span 500 μm), while right column images were acquired at high magnification (black bars span 200 μm). (a–b) group #2 (matrix and hMSC); (c–d) group #3 (matrix and hrBMP-7); (e–f) group #4 (matrix, hMSC and hrBMP-7); (g–h) group #5 (matrix, cADPR-pre-treated hMSC and hrBMP-7). **1** Orthoss® particle; **2** connective tissue; **3** new bone; 4 bone marrow. Panel B: quantification of the areas of Orthoss®, connective tissue, new bone and bone marrow present in the histological sections (2 per animal, 6 animals per group) obtained from experimental groups #2, 3, 4 and 5. Tissue areas were quantified on low magnification images (as in panel A, left column) with the Adobe Photoshop 7.0 Professional software. Tissue areas are expressed as percentages ± SD of the total area of the transplant in the femoral gap.

rejection of the transplanted cells. In this CSSBD rat model, a minimum of 2×10^6 hMSC, in the presence of hrBMP-7, was necessary to observe significant bone regeneration and a higher number of cells did not result in an increased bone formation (Fig. 3). The fact that increasing the number of hMSC or the dose of BMP-7 in the graft did not results in bone overgrowth at the CSSBD (see Results) should minimize the risk of excess callus formation in the clinical setting, due to overdosage of either cells or BMP-7. Five experimental groups were tested: group #1 received matrix alone (Orthoss®), group #2 received the matrix and in vitro-expanded hMSC, group #3 received the matrix and hrBMP-7, group #4 received the matrix, hMSC and hrBMP-7 and group #5 received the matrix, hrBMP-7 and hMSC cultured for the last 48 h with the Ca^{2+}-mobilising second messenger cADPR, which stimulates hMSC proliferation [16]. All the evaluations performed postoperatively to assess bone regeneration, i.e. X-ray (Fig. 4), μCT (Fig. 5) and histological analysis of the regenerated bone (Fig. 6), consistently indicated that groups #4 and #5 scored better than the other groups. In particular, groups #4 and #5 received a radiographic evaluation score $\geq$3, had the highest percentage of new bone formation (approx. 30%), and a higher percentage of matrix resorption, suggesting that mechanisms of active substitution of Orthoss® particles with new bone were underway. The failure by hMSC alone to regenerate the bone tissue in our model is in contrast with results obtained by Nakamura et al. [30], who observed successful femur nonunion repair using a sheet of rat MSC in the absence of matrix; in this case, however, the bone defect was significantly smaller. In the CSSBD model used in this study, the important role of the matrix in the bone regeneration process in groups #4 and 5 is indicated by the fact that newly formed bone can be observed only around the Orthoss® particles (Fig. 6F and H). The improved healing resulting from the combination of hMSC with BMP-7 as compared to treatment with either one or the other may be due to, i) the increased osteogenic differentiation of implanted hMSC, or, ii) the induction by BMP-7 of the transcription and release of growth and differentiation factors by implanted hMSC (15), improving endogenous bone regeneration by rat cells.

Pre-treatment of hMSC for 48 h with cADPR prior to transplantation resulted in an approx. 40% increase of the cell number compared to untreated cultures (Fig. 1), in line with published observations [16]. The fact that addition of hrBMP-7 resulted in a similar slight reduction of the cell number in cADPR-treated and -untreated cells suggests that cADPR-expanded hMSC remain sensitive to the induction of differentiation by hrBMP-7. This conclusion is sustained also by the observation of a similar increase of Runx2, ALP and OP expression compared to untreated controls in differentiated hMSC treated with hrBMP-7 alone or with hrBMP-7 in combination with cADPR (Fig. 2, white bars). Finally, in the *in vivo* CSSBD model, the group receiving cADPR-pre-treated hMSC (group #5) scored similarly in all postoperative analyses compared to animals transplanted with cADPR-untreated hMSC (group #4, Figs. 4–6). Altogether, these results indicate that the *in vitro* expansion of hMSC with cADPR accelerates cell proliferation without affecting the differentiation and bone regenerating ability of hMSC and may thus be employed to shorten the *in vitro* expansion time preceding cell transplant. The fact that both *in vitro* expanded human hMSC and the BMP-7 preparation used in this study are already separately in clinical use should expedite the possible approval for their combined use for the treatment of CSSBD in humans.

Acknowledgments

This work was supported by grants from: Regione Liguria (CIPE Project, Stem Cells Area), MIUR PRIN project 2007BZ4RX3, MIUR FIRB projects RBAUO19A3C, RBNE01ERXR, RBLAD39LSF, RBIP06LSS2, University of Genova, Italian Ministry of Health (PRF/2004), Fondazione CARIGE and Fondazione "Livio Sciutto." The authors acknowledge Geistlich Biomaterials for kindly providing Orthoss® particles. The authors are deeply indebted to Prof. Antonio De Flora for his scientific support and valuable discussions, and they are also grateful to Cristian Piana and Alessio Ferraro for their help during this work.

References

[1] Asada N, Tsuchiya H, Kitaoka K, Mori Y, Tomita K. Massive autoclaved allografts and autografts for limb salvage surgery. A 1-8 year follow-up of 23 patients. Acta Orthop Scand 1997;68:392–5.
[2] Krampera M, Pizzolo G, Aprili G, Franchini M. Mesenchymal stem cells for bone, cartilage, tendon and skeletal muscle repair. Bone 2006;39:678–83.
[3] Pittenger MF, Mackay AM, Beck SC, Jaiswal RK, Douglas R, Mosca JD, Moorman MA, Simonetti DW, Craig S, Marshak DR. Multilineage potential of adult human mesenchymal stem cells. Science 1999;284:143–7.
[4] Krebsbach PH, Kuznetsov SA, Satomura K, Emmons RV, Rowe DW, Robey PG. Bone formation in vivo: comparison of osteogenesis by transplanted mouse and human marrow stromal fibroblasts. Transplantation 1997;63:1059–69.
[5] Kon E, Muraglia A, Corsi A, Bianco P, Marcacci M, Martin I, Boyde A, Ruspantini I, Chistolini P, Rocca M, Giardino R, Cancedda R, Quarto R. Autologous bone marrow stromal cells loaded onto porous hydroxyapatite ceramic accelerate bone repair in critical-size defects of sheep long bones. J Biomed Mater Res 2000;49:328–37.
[6] Petite H, Viateau V, Bensaid W, Meunier A, de Pollak C, Bourguignon M, Oudina K, Sedel L, Guillemin G. Tissue-engineered bone regeneration. Nat Biotechnol 2000;18:959–63.
[7] Bruder SP, Kurth AA, Shea M, Hayes WC, Jaiswal N, Kadiyal S. Bone regeneration by implantation of purified, culture-expanded human mesenchymal stem cells. J Orthop Res 1998;16:155–62.
[8] Quarto R, Mastrogiacomo M, Cancedda R, Kutepov SM, Mukhachev V, Lavroukov A, Kon E, Marcacci M. Repair of large bone defects with the use of autologous bone marrow stromal cells. N Engl J Med 2001;344(5):385–6.
[9] European Commission-Health and Consumer Protection Directorate General. Technical requirements for the coding, processing, preservation storage and distribution of human tissues and cells. Directive 2004/23/EC.
[10] Vacanti JP, Langer R. Tissue engineering; the design and fabrication of living replacement devices for surgical reconstruction and transplantation. Lancet 1999;354(Suppl 1):S132–4.
[11] Schwarz F, Ferrari D, Sager M, Herten M, Hartig B, Becker J. Guided bone regeneration using rhGDF-5- and rhBMP-2-coated natural bone mineral in rat calvarial defects. Clin Oral Implants Res 2009;20:1219–30.
[12] Deng F, Ling J, Ma J, Liu C, Zhang W. Stimulation of intramembranous bone repair in rats by ghrelin. Exp Physiol 2008;93(7):872–9.
[13] Kim SS, Kim BS. Comparison of osteogenic potential between apatite-coated poly (lactide-co-glycolide)/hydroxyapatite particulates and Orthoss. Dent Mater J 2008;27(3):368–75.
[14] Gautschi OP, Frey SP, Zellweger R. Bone morphogenetic proteins in clinical applications. ANZ J Surg 2007;77:626–31.
[15] Lavery K, Hawley S, Swain P, Rooney R, Falb D, Alaoui-Ismaili MH. New insights into BMP-7 mediated osteoblastic differentiation of primary human mesenchymal stem cells. Bone 2009;45:27–41.
[16] Scarfì S, Ferraris C, Fruscione F, Fresia C, Guida L, Bruzzone S, Usai C, Parodi A, Millo E, Salis A, Burastero G, De Flora A, Zocchi E. Cyclic ADP-ribose-mediated expansion and stimulation of human mesenchymal stem cells by the plant hormone abscisic acid. Stem Cells 2008;26(11):2855–64.
[17] Pozzolini M, Scarfì S, Benatti U, Giovine M. Interference on MTT cell viability assay in activated macrophage cell line. Anal Biochem 2003;313:338–41.
[18] Tichopad A, Dilger M, Schwarz G, Pfaffl MW. Standardized determination of real-time PCR efficiency from a single reaction set-up. Nucleic Acids Res 2003;31:e122.
[19] Pfaffl MW. A new mathematical model for relative quantification in real-time RT-PCR. Nucleic Acids Res 2001;29:e45.
[20] Cook SD, Barrack RL, Santman M, Patron LP, Salkeld SL, Whitecloud III TS. The Otto Aufranc Award. Strut allograft healing to the femur with recombinant human osteogenic protein-1. Clin Orthop Relat Res 2000;381:47–57.
[21] Donath K, Breuner G. A method for the study of undecalcified bones and teeth with attached soft tissues. The Säge-Schliff (sawing and grinding) technique. J Oral Pathol 1982;11(4):318–26.
[22] Chen TL, Shen WJ, Kraemer FB. Human BMP-7/OP-1 induces the growth and differentiation of adipocytes and osteoblasts in bone marrow stromal cell cultures. J Cell Biochem 2001;82:187–99.
[23] Andrades JA, Santamaria JA, Nimdni ME, Becerra J. Selection and amplification of a bone marrow cell population and its induction to the chondro-osteogenic lineage by rhOP-1: an in vitro and in vivo study. Int J Dev Biol 2001;45:689–93.
[24] Klein-Nulend J, Louwerse RT, Heyligers IC, Wuisman PI, Semeins CM, Goei SW, Burger EH. Osteogenic protein (OP-1, BMP-7) stimulates cartilage differentiation of human and goat perichondrium tissue in vitro. J Biomed Mater Res 1993;40:614–20.
[25] Thomson BM, Bennett J, Dean V, Triffitt J, Meikle MC, Loveridge N. Preliminary characterization of porcine bone marrow stromal cells: skeletogenic potential, colony forming activity and response to dexamethasone, transforming growth factor beta and basic fibroblast growth factor. J Bone Miner Res 1993;8:1173–83.
[26] Cook SD, Baffes GC, Wolfe MW, Sampath TK, Rueger DC. Recombinant human bone morphogenetic protein-7 induces healing in a canine long-bone segmental defect. Clin Orthop Relat Res 1994;301:302–12.

[27] den Boer C, Bramer JA, Blokhuis TJ, Van Soest EJ, Jenner JM, Patka P, Bakker FC, Burger EH, Haarman HJ. Effect of recombinant human osteogenic protein-1 on the healing of a freshly closed diaphyseal fracture. Bone 2002;31:158–64.
[28] Friedlaender GE, Perry CR, Cole JD, Cook SD, Cierny G, Muschler GF, Zych GA, Calhoun JH, LaForte AJ, Yin S. Osteogenic protein-1 (bone morphogenetic protein-7) in the treatment of tibial nonunions. J Bone Joint Surg Am 2001;83(Suppl 1):S151–8.
[29] Poynton AR, Lane JM. Safety profile for the clinical use of bone morphogenetic proteins in the spine. Spine 2002;27(Suppl 1):S40–8.
[30] Nakamura A, Akahane M, Shigematsu H, Tadokoro M, Ohgushi H, Dohi Y, Imamura T, Tanaka Y. Cell sheet transplantation of cultured mesenchymal stem cells enhances bone formation in a rat nonunion model. Bone 2010;46: 418–24.